Sublimation of Graphite at Hypersonic Speeds

SINCLAIRE M. SCALA* AND LEON M. GILBERT†
General Electric Company, Philadelphia, Pa.

In this paper, a new theoretical model is presented for the sublimation of graphite at hypersonic flight speeds. The aerothermochemical interactions between dissociated air and graphite are treated by means of a nine-component model, including O, O_2, N, N_2, CO, CO_2, C, C_3, and CN. The mass-transfer rate, the heat-transfer rate, and the skin-friction coefficient are determined numerically and are then correlated by means of algebraic equations as a function of stagnation pressure, stagnation enthalpy, and wall temperature in the high-Reynolds-number stagnation-point flow regime.

Nomenclature

Å	=	angstroms
B_i	=	referred mole fraction of species i, $X_i/\bar{M}$
C_i	=	mass fraction of species i
$C_{\langle k \rangle}$	=	effective mass fraction of kth chemical element
C_{p_i}	=	specific heat of ith species at constant pressure
$\bar{C}_p$	=	frozen specific heat of mixture
$\mathfrak{D}_{ij}$	=	binary diffusion coefficient
D_{ij}	=	multicomponent diffusion coefficient
E	=	activation energy
f	=	dimensionless stream function
H	=	stagnation enthalpy
h_i	=	static enthalpy of ith species, including chemical
h	=	static enthalpy of mixture $= \sum_i C_i h_i$
$\Delta h_{0_{f_i}}$	=	enthalpy of formation of ith species
$\mathbf{j}$	=	diffusion flux vector, defined in Eq. (27)
k	=	Boltzmann constant
K	=	frozen thermal conductivity of mixture
K_0	=	effective collision frequency
K_p	=	equilibrium constant
M_i	=	molecular weight of species i
$\bar{M}$	=	mean molecular weight of gas mixture
$\dot{m}_i$	=	mass flux of species i
P	=	static gas pressure
Q	=	heat transfer
R	=	universal gas constant
R_B	=	body radius
T	=	temperature
u, v	=	velocity components
v	=	macroscopic gas velocity
V_i	=	diffusion velocity of species i
V_∞	=	flight speed
$\dot{w}_i$	=	chemical source term, net mass rate of production of species i per unit volume by chemical reaction
X_i	=	mole fraction of species i
x, y, r	=	coordinate system
β	=	pressure gradient parameter, $2d \ln u_e/d \ln \xi$
ϵ	=	normal shock-density ratio, depth of potential well
η, ξ	=	similarity variables
$\theta = T/T_e$	=	dimensionless temperature
μ_i	=	viscosity of ith species
ρ	=	density
σ	=	collision diameter
τ	=	shear stress
φ	=	property of element k, pertains to C, $\mathbf{j}$, $\dot{m}$, and $\dot{w}$

Subscripts

D	=	diffusion-controlled oxidation regime
e	=	edge of viscous layer
g	=	gas
i	=	ith species
k	=	kth element
mix	=	mixture
s	=	stagnation region, condensed phase, sublimation regime
R	=	reaction-rate-controlled regime
w	=	wall, surface of vehicle
η	=	differentiation with respect to η

Dimensionless Groups

B	=	$\dot{m}_w(H_e - h_w)/Q_w$
C_H	=	$Q_w/\rho_e u_e(H_e - h_w)$, Stanton number
C_f	=	$2\tau_w/\rho_e u_e^2$, skin-friction coefficient
l	=	$\rho\mu/\rho_w\mu_w$
L_{ij}	=	$\rho\bar{C}_p D_{ij}/K$, multicomponent Lewis number
Pr	=	$\mu\bar{C}_p/K$, Prandtl number
Re_s	=	$\rho_\infty V_\infty R_B/\mu_e$, shock Reynolds number

Presented at the AIAA Entry Technology Conference, Williamsburg and Hampton, Va., October, 12–14, 1964 (no preprint number; published in bound volume of preprints of the meeting); based on General Electric Company Report TIS R 64 SD 55, revision received April 19, 1965. This paper is based on work performed under the auspices of the United States Air Force, Ballistic System Division, Contracts No. AF 04(647)-269 and No. AF 04(694)-222. The authors are pleased to acknowledge the discussions of surface kinetics held with Peter Zavitsanos and Bernard Hamel of the General Electric Company Space Sciences Laboratory. The first author also wishes to acknowledge the discussion with Daniel Rosner of the Aero Chem Research Laboratories on the concept of resistances in series that led to the derivation of Eq. (39). The differential equations were programed for digital computations on the IBM 7094 by Frank Bosworth and James Massey.

* Manager, Theoretical Fluid Physics, Space Sciences Laboratory. Associate Fellow Member AIAA.

†Thermophysicist, Space Sciences Laboratory. Member AIAA.

I. Introduction

IN a sequence of earlier theoretical studies, the combustion of graphite was treated in the diffusion-controlled regime[1–3] and in the rate-controlled and transition regimes.[3] These results were utilized in considering the ablation response of a graphite heat shield for a ballistic re-entry satellite[2–4] and the transient thermochemical response of a pyrolytic graphite leading edge for the control surface of a hypersonic lifting re-entry vehicle.[5,6] The studies carried out to date indicate that, in general, the mass loss depends upon the surface temperature, the pressure, enthalpy, and chemical reactivity of the gaseous boundary layer, the flow geometry, and the chemical reactivity of the particular type of carbon considered.

At the lowest surface temperatures ($T_w \sim 1500°$R), the reaction of carbon with oxygen results in the formation of both carbon monoxide and carbon dioxide at active sites in the surface lattice. The number of such active sites is a strong function of surface temperature, whereas the coverage of these sites by freestream oxygen depends upon the local ambient pressure and the gas particle temperature. It should be noted that there is also a possibility of interaction between the microstructure of the carbonaceous material (such as pores) and the adsorbed monolayer that could alter the apparent order of the chemical reaction. However, in the absence of pores, the mass loss should be zeroth order

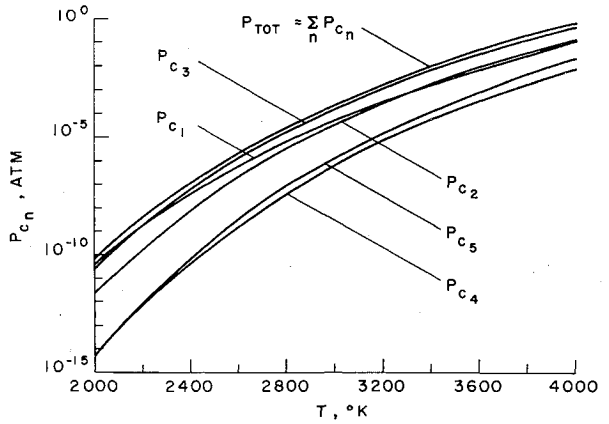

Fig. 1 Partial pressures of vaporized species for graphite sublimation.

initially, since the monolayer is not depleted rapidly by the active sites.

At a somewhat higher surface temperature, the number of active sites begins to increase exponentially. If the mass loss in the reaction-rate-controlled regime were dependent only upon the arrival of oxygen or oxygen-bearing species and the coverage of the active sites in the lattice, one would expect the over-all order of the reaction to be first order in the pressure. However, experimental data have been reported for this regime covering a range of reaction orders from zero to one,[7,8] and, in some cases, one-half has been recommended.[9,10]

It also has been observed[11] that, as the surface temperature rises, the ratio of the mass fraction of carbon monoxide to that of carbon dioxide at the surface increases exponentially which may be explained in terms of a heterogeneous chemical reaction between CO_2 and $C(s)$ to form CO. Here, it is noted that the formation of CO at the surface could follow a complex sequence of steps including adsorption, dissociation, formation of one or more chemical complexes, and desorption of two CO molecules.

As the surface temperature rises still further ($T_w \sim$ 2000°R), there is a transition from the reaction rate to the diffusion-controlled oxidation regime. In this transition regime, the rate of mass loss is controlled by both fluid dynamic and chemical kinetic rate processes.[3,12,13] For a range of surface temperatures approximately between 2500° and 5000°R, the rate of the over-all mass loss is dominated by the slowest step, which is the counterdiffusion process in the multicomponent boundary layer.[3]

In this present study, we are concerned with even higher surface temperatures ($T_w \geq$ 5000°R), i.e., the sublimation regime. We define the sublimation regime as the range of conditions where the mass loss caused by vaporization exceeds the diffusion-controlled oxidation mass loss rate. It is noted

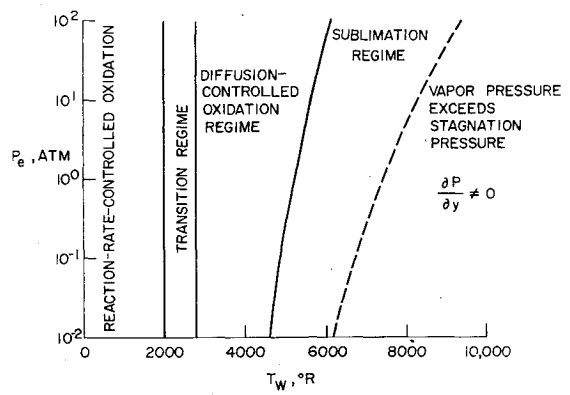

Fig. 2 Mass-transfer regimes for ablating graphite.

that, at the high surface temperatures to be treated here, i.e., 5000°R $< T_w <$ 10,000°R, not only do chemical reactions occur between carbon and oxygen, but also, nitrogen reacts with carbon to form cyanogen $(CN)_2$ and the cyano radical CN. We must be concerned therefore with both the homogeneous and heterogeneous chemical reactions involving the nitrogen, which is present in the boundary layer. As the surface temperature rises, the vaporization rate of atomic and molecular carbon species, such as C, C_2, C_3, C_4, and C_5, all increase exponentially. Upon examination of the thermodynamic properties and the vaporization-rate data (Fig. 1), of Vidale,[14] the authors have selected a nine-component gas model to represent the aerothermochemical interactions, i.e., O, O_2, N, N_2, CO, CO_2, C, C_3, and CN.

The decision concerning the number of chemical species to be included in the model represents a compromise between reality and computational ease. Too many can make the problem unwieldy; too few results in a poor physical representation. Our approach, therefore, has been to include all of the dominant species and a few of the trace species. By dominant is meant all of those species, which contribute 5% or more to the total gas enthalpy at a point in the stream. The presence of the species NO, $(CN)_2$, and C_2 has been neglected therefore.

The present theoretical model depends upon the validity of the boundary-layer approximation, which requires that $(\partial P/\partial y) = 0$. Since the sum of the partial pressures of the vaporizing species increases exponentially with surface temperature, there will be some critical surface temperature at each value of the stagnation pressure where the present results begin to become invalid because of the presence of a pressure gradient normal to the surface (Fig. 2).

It is noted that an earlier solution to the problem of the sublimation of graphite at hypersonic speeds was obtained by Denison and Dooley,[15] who utilized the constant-property boundary-layer equations for a flat plate and the Emmons and Leigh[16] correlation between skin friction and mass transfer on a flat plate to obtain numerical results. However, since they restricted their chemical model to include only six species (i.e., the presence of CO_2, C_3, and CN was neglected) and since a large number of assumptions was introduced in order to reduce the general equations to the constant-property, flat-plate form, thereby avoiding new digital computations, their final numerical results differ appreciably from ours.

In a treatment of sublimation into a boundary layer, it is important to note that the over-all mass loss may be either an "equilibrium" process or a nonequilibrium process.[17] Associated with each vaporizing species is a vaporization coefficient, which is a measure of the rate of forward vaporization of that species.[17] However, the vaporization coefficients alone do not determine whether the over-all process will be diffusion-controlled equilibrium vaporization or a nonequilibrium process, which depends upon the coupling between the forward rate of vaporization and the aerodynamic processes in the boundary layer.

In the present study, we will assume that "equilibrium vaporization" applies, i.e., the net mass loss, because of diffusion and convection, is very small as compared to the

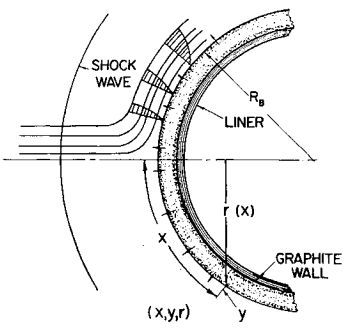

Fig. 3 Coordinate system.

forward rate of vaporization. Thus, the condensation rate and the vaporization rate are nearly equal, and the sum of the partial pressures, within a mean free path from the surface, is nearly equal to the equilibrium vapor pressure.

If on the other hand, the ambient pressure is very low, and if the vaporization coefficients are very small,[17] then any finite net mass loss by diffusion and convection in the boundary layer results in a reduction in the individual partial pressures of the vaporizing species below their equilibrium vapor-pressure values. In this case, the net mass loss cannot be determined from a knowledge of the equilibrium vapor pressures alone, since the driving force for diffusion and convection is now the nonequilibrium partial pressure of the vaporizing species. One then must determine the partial pressures of the vaporizing species by utilizing compatibility constraints caused by gas kinetic microscopic and fluid mechanic macroscopic considerations.[18]

II. Conservation Laws

The equations for the conservation of mass, chemical species, momentum, and energy[19] for the axisymmetric stagnation-region boundary layer[20] (Fig. 3) are

$$(\partial/\partial x)(\rho r u) + (\partial/\partial y)(\rho r v) = 0 \tag{1}$$

The conservation equation for species i becomes (neglecting thermal diffusion and other higher-order effects)

$$\rho M_i \left(u\frac{\partial B_i}{\partial x} + v\frac{\partial B_i}{\partial y}\right) + \frac{\partial}{\partial y}\left[\sum_{j\neq i}\frac{M_i M_j}{\bar{M}^2}\rho D_{ij}\frac{\partial X_j}{\partial y}\right] = \dot{w}_i \tag{2}$$

The streamwise component of momentum yields

$$\rho u\frac{\partial u}{\partial x} + \rho v\frac{\partial u}{\partial y} = -\frac{\partial P}{\partial x} + \frac{\partial}{\partial y}\left(\mu\frac{\partial u}{\partial y}\right) \tag{3}$$

In the high-Reynolds-number regime, for moderately high mass-transfer rates, we may write that the normal component of momentum yields

$$\partial P/\partial y = 0 \tag{4}$$

In this study, criteria are developed for determining the conditions when Eq. (4) no longer applies (Fig. 2). The energy equation becomes

$$\rho\bar{C}_p\left(u\frac{\partial T}{\partial x} + v\frac{\partial T}{\partial y}\right) = u\frac{\partial P}{\partial x} + \mu\left(\frac{\partial u}{\partial y}\right)^2 + \frac{\partial}{\partial y}\left(K\frac{\partial T}{\partial y}\right) - \sum_i C_{pi}\frac{\partial T}{\partial y}\sum_{j\neq i}\frac{M_i M_j}{\bar{M}^2}\rho D_{ij}\frac{\partial X_j}{\partial y} - \sum_i \dot{w}_i h_i \tag{5}$$

where the equation of state is $P = \rho R\bar{M}^{-1}T$.

It is convenient to introduce the Mangler-Dorodnitsyn transformation[21] in solving these laminar boundary-layer equations:

$$\eta = \frac{\rho_e u_e}{(2\xi)^{1/2}}\int_0^y r\frac{\rho}{\rho_e}dy \tag{6}$$

$$\xi = \int_0^x \rho_w\mu_w u_e r^2 dx \tag{7}$$

At the stagnation point, Eqs. (1–5) are reduced to a set of ordinary nonlinear differential equations. The diffusion equation for the ith chemical species becomes

$$\left[\frac{l}{Pr}\sum_{j\neq i}\frac{M_i M_j}{\bar{M}^2}L_{ij}X_{j\eta}\right]_\eta - fM_i B_{i\eta} = \frac{\beta}{(du_e/dx)}\frac{\dot{w}_i}{\rho} \tag{8}$$

The conservation of momentum becomes

$$(lf_{\eta\eta})_\eta + ff_{\eta\eta} + \beta[(\rho_e/\rho) - f_\eta^2] = 0 \tag{9}$$

The energy equation becomes

$$\left(\frac{\bar{C}_p l}{Pr}\theta_\eta\right)_\eta + \bar{C}_p f\theta_\eta - \sum_i\frac{C_{pi}l}{Pr}\theta_\eta\sum_{j\neq i}\frac{M_i M_j}{\bar{M}^2}L_{ij}X_{j\eta} + \frac{u_e^2}{T_e}\left[l(f_{\eta\eta})^2 + \beta f_\eta\left(\theta - \frac{\rho_e}{\rho}\right)\right] = \frac{\beta}{(du_e/dx)}\frac{\sum_i \dot{w}_i h_i}{\rho T_e} \tag{10}$$

III. Transport and Thermodynamic Properties

Appearing in Eqs. (8–10) are the variable coefficients, which represent the thermodynamic properties and transport coefficients of the gas mixture. The details concerning the calculation of the transport and thermodynamic properties of the pure species and also the bulk properties of a multicomponent, chemically reacting gas mixture are given in Ref. 19.

The low-temperature properties utilized in this sublimation study have been given in Ref. 3. The properties of the additional species included in this study (i.e., C, C_3, and CN) and also the new resulting binary interactions are shown in Figs. 4–8. The gas constants used for these calculations are assembled in Table 1.

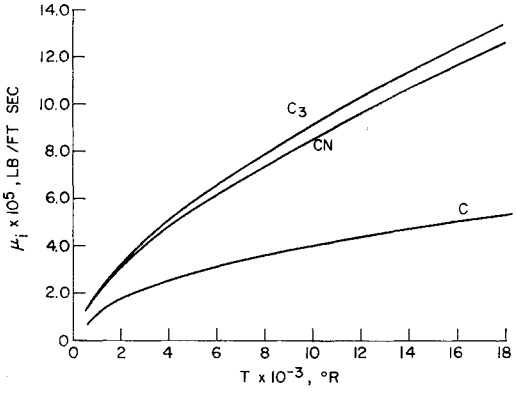

Fig. 4 Viscosity coefficients.

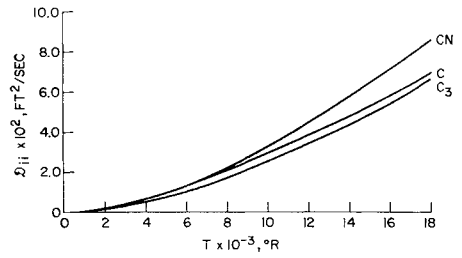

Fig. 5 Self-diffusion coefficients, p = 1.0 atm.

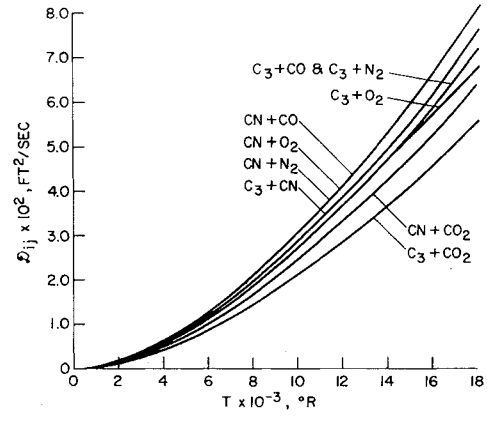

Fig. 6 Binary diffusion coefficients, Lennard-Jones (6-12) potential, p = 1.0 atm.

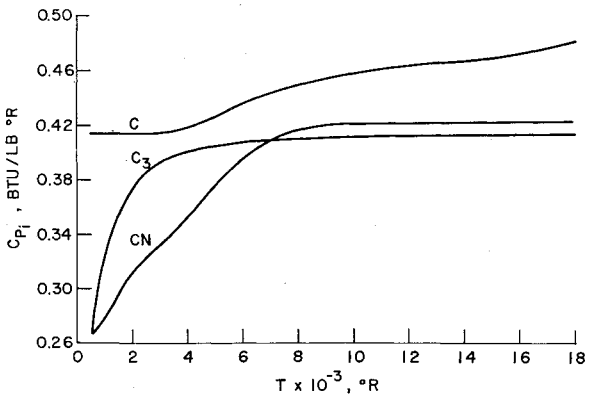

Fig. 7 Specific heat vs temperature.

Of course, great numerical simplifications result if one assumes that the Prandtl and Lewis numbers remain constant throughout the viscous layer. We have made a comparison of a constant-property solution with a variable-property solution, as applied to the graphite sublimation problem. In the constant-property solution, the Prandtl number of the mixture and the multicomponent Lewis numbers were evaluated at the surface conditions. However, the viscosity of the mixture and all of the thermodynamic coefficients were evaluated locally throughout the viscous layer for both cases. Excellent agreement between the two was obtained.

IV. Chemical Constraints

Since the total number of dominant species present is nine, there are nine unknown chemical source terms $\dot{w}_i$ and nine unknown concentrations X_i at each point in the gas. At the surface, there are nine unknown concentrations, which must satisfy the chemical constraints imposed by the heterogeneous kinetics of the gas-solid interactions and also must be compatible with the gas-phase diffusion processes. At the outer edge of the boundary layer, the gas state is obtained from the solution of the normal shock equations, followed by an isentropic compression along the stagnation streamline.[23]

An obvious chemical constraint is the conservation of individual chemical elements. We therefore find it convenient to introduce the following notation for the relationship between the required properties of the elements ⟨O⟩, ⟨N⟩, and ⟨C⟩ in terms of the properties of the nine species:

$$\varphi_{\langle O\rangle} = \varphi_O + \varphi_{O_2} + (M_O/M_{CO})\varphi_{CO} + (M_{O_2}/M_{CO_2})\varphi_{CO_2} \quad (11)$$

$$\varphi_{\langle N\rangle} = \varphi_N + \varphi_{N_2} + (M_N/M_{CN})\varphi_{CN} \quad (12)$$

$$\varphi_{\langle C\rangle} = \varphi_C + \varphi_{C_3} + M_C\left[\frac{\varphi_{CO}}{M_{CO}} + \frac{\varphi_{CO_2}}{M_{CO_2}} + \frac{\varphi_{CN}}{M_{CN}}\right] \quad (13)$$

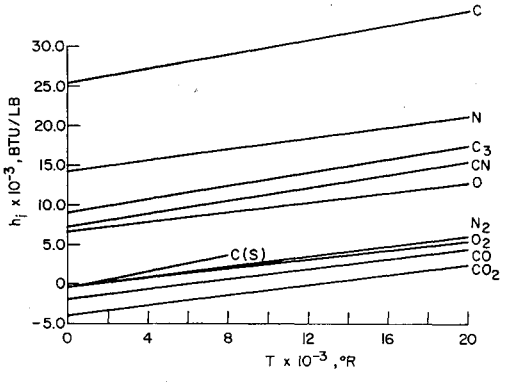

Fig. 8 Enthalpy of pure species for graphite ablation.

In terms of the preceding notation, we may immediately write

$$\dot{w}_{\langle O\rangle} = 0 \qquad \dot{w}_{\langle N\rangle} = 0 \qquad \dot{w}_{\langle C\rangle} = 0 \quad (14)$$

where $\dot{w}_{\langle k\rangle}$ is defined by $\varphi_{\langle k\rangle}$. The expression for the over-all conservation of mass is obtained by adding Eqs. (14):

$$\sum_i \dot{w}_i = 0 \quad (15)$$

To complete the analysis of the gas-phase chemistry, it is noted that, in addition to Eqs. (14), six relationships still are needed which specify the rates of the chemical reactions. For the assumption of local thermochemical equilibrium, one has the necessary information from the first six equations appearing in Table 2. These equilibrium functions, of course, include all of the possible equilibrium chemical reactions between the nine species treated here.

Now let us turn our attention to the chemical interactions at the gas-solid interface. In order to define the system completely, three additional relationships are required. One of these will be an equilibrium function, applicable only at the surface. Another condition is obtained from Dalton's law of partial pressures, and for the final relationship, we make use of the fact that, physically, the surface is impermeable to the mass fluxes of the elements oxygen and nitrogen. The chemical reaction, and the corresponding equilibrium function, which applies only at the wall is Eq. (22) in Table 2. Equation (22), when used in combination with Eqs. (16–21), allows one to determine all of the possible gas-surface interactions for this system. From Dalton's law, we obtain the information that the sum of the mole fractions equals unity. For the final condition, which results in a mass flux compatibility constraint, we make use of the following impermeability conditions:

$$\dot{m}_{\langle N\rangle_w} = 0 \qquad \dot{m}_{\langle O\rangle_w} = 0 \quad (23)$$

where $\dot{m}_{\langle k\rangle}$ is defined by $\varphi_{\langle k\rangle}$ [see Eqs. (11–13)]. Using the fact that

$$\dot{m}_{i_w} = C_{i_w}\dot{m}_w + j_{i_w} \quad (24)$$

one then obtains

$$(j_{\langle N\rangle}/C_{\langle N\rangle})_w = (j_{\langle O\rangle}/C_{\langle O\rangle})_w \quad (25)$$

where $j_{\langle k\rangle}$ and $C_{\langle k\rangle}$ are defined by $\varphi_{\langle k\rangle}$, which is the mass flux compatibility constraint.

The surface mass transfer is caused by the mass flux of the element carbon, and introducing Eq. (24),

$$\dot{m}_w = \dot{m}_{\langle C\rangle_w} = [j_{\langle C\rangle}/(1 - C_{\langle C\rangle})]_w \quad (26)$$

The multicomponent diffusion flux vector $\mathbf{j}_i$ utilized in this study is given as follows:

$$\mathbf{j}_i = \rho_i\mathbf{V}_i = \rho\bar{M}^{-2}\sum_{j\neq i} M_iM_jD_{ij}\nabla X_j \quad (27)$$

Note that in the preceding equation the effects of thermal diffusion, pressure gradients, and body forces are neglected, and the D_{ij} are the multicomponent diffusion coefficients.

Table 1 Gas constants, $T_{Ref.} = 540°R$

Species	σ_i, A	M_i	$(\epsilon/k)_i$, °K	$\Delta h_{f_i}°$, Btu/lb
O	2.96	16	...	6,654
O_2	3.54	32	88.0	0
N	2.88	14	...	14,527
N_2	3.749	28	79.8	0
CO	3.59	28	110.0	−1,698
CO_2	3.897	44	213.0	−3,848
C	3.42	12	...	25,755
C_3	3.6	36	150	9,517
CN	3.5	26	115	7,689

Table 2 Equilibrium constants, $\log_{10}K_p = a - b/T$, °R

Eq. no.	Reaction	Equilibrium constant, P_i is in atm	a	$b \times 10^{-4}$
16	$O_2 \rightleftarrows 2O$	$K_{p_O} = P_O^2/P_{O_2}$	6.80	4.68
17	$N_2 \rightleftarrows 2N$	$K_{p_N} = P_N^2/P_{N_2}$	7.00	9.00
18	$CO + O \rightleftarrows CO_2$	$K_{p_{CO_2}} = P_{CO_2}/P_{CO}P_O$	−8.00	−5.04
19	$C + O \rightleftarrows CO$	$K_{p_{CO}} = P_{CO}/P_CP_O$	−7.43	−10.29
20	$C + N \rightleftarrows CN$	$K_{p_{CN}} = P_{CN}/P_CP_N$	−6.63	−7.59
21	$3C \rightleftarrows C_3$	$K_{p_{C_3}} = P_{C_3}/P_C^3$	−14.77	−12.83
22	$C(s) \rightleftarrows C$	$K_{p_C} = P_C$	8.12	6.69

V. Boundary Conditions

In general, the over-all mathematical order of the high Reynolds number, thin boundary-layer system is $2n + 3$, where n is the number of chemical species in the gas mixture. Five boundary conditions are applied to the energy and momentum equations. At the wall,

$$\theta_w = T_w/T_e \tag{28}$$

$$f_{\eta_w} = u_w/u_e = 0 \tag{29}$$

$$-f_w = \dot{m}_w[\rho_w\mu_w(du_e/dx)/\beta]^{-1/2} \tag{30}$$

and at the outer edge of the boundary layer, the temperature and velocity go to their asymptotic limits:

$$\lim_{\eta \to \infty} \theta = \lim_{\eta \to \infty} f_\eta = 1.0 \tag{31}$$

The differential equations are solved numerically by iterating on θ_{η_w} and $f_{\eta\eta_w}$ until boundary conditions (31) are satisfied. The remaining $2(n - 1)$ boundary conditions deal with the chemical species. For an n component gas mixture, in which there are k chemical elements, $2(k - 1)$ chemical mass balance and mass flux relationships must be satisfied. This leaves $2(n - k)$ relationships, which deal with the rates at which the chemical reactions are progressing.

If the chemical reaction times are much shorter than the flow rate times, then a state of local thermochemical equilibrium exists in the gas phase. For this situation, the chemical equilibrium (K_p) functions and their derivatives satisfy these $2(n - k)$ relationships. Therefore the equilibrium assumption reduces the over-all mathematical order of the system from $(2n + 3)$ to $(2k + 3)$, where five boundary conditions are applied to the energy and momentum equations, and the remaining $2(k - 1)$ boundary conditions deal with the remaining chemical mass balance and mass flux relationships. For the particular case, which we treat here (i.e., equilibrium graphite sublimation), $n = 9$, $k = 3$, and the six K_p functions are given by Eqs. (16–21).

At the outer edge of the boundary layer, the concentrations of the carbon-bearing species individually go to zero, and the ratio of the masses of the elements oxygen to nitrogen takes on its freestream value:

$$C_{\langle C \rangle_e} = 0 \qquad (C_{\langle O \rangle}/C_{\langle N \rangle})_e = 0.3068 \tag{32}$$

Within the viscous layer, the lighter-weight particles tend to diffuse faster than the heavier ones which results in preferential diffusion; hence, the ratio of the masses of the elements oxygen to nitrogen does not remain constant throughout the boundary layer. Therefore, one makes use of the surface impermeability conditions [i.e., Eqs. (23)], which result in the surface mass flux compatibility constraint given by Eq. (25). Finally, the rate at which the gaseous element carbon is produced from the solid phase is given by Eq. (22), used in conjunction with the other K_p functions.

In the numerical integration of the differential equations $(C_{\langle O \rangle}/C_{\langle N \rangle})_w$ and $-f_w$ are specified and are iterated upon until the boundary conditions (32) are satisfied. To summarize, the five boundary conditions at the wall for the equilibrium situation are given by Eqs. (22, 25, 26, 28, and 29), and the four eigenvalues at the wall ($\eta = 0$) are θ_{η_w}, $f_{\eta\eta_w}$, $-f_w$, and $(C_{\langle O \rangle}/C_{\langle N \rangle})_w$. The total number of boundary conditions and eigenvalues at the surface is therefore $2k + 3 = 9$ which is the true mathematical order of the system for the "equilibrium" case.

VI. Discussion of Results

The chemical composition at a graphite surface in a hypersonic air stream is shown in Fig. 9 for a range of surface temperatures at a stagnation pressure of 1 atm. Similar results are obtained at other pressures. Increasing the pressure causes a shift in the composition variation seen here to a high-temperature range, whereas lower pressures result in a displacement toward lower temperatures.

The concentrations of the chemical species O, N, O_2, and CO_2 are found to be less than 10^{-4} over the full range of surface temperatures at a pressure of 1 atm. It is seen that nitrogen begins to react with the graphite surface at a surface temperature of approximately 5000°R, whereas the sublimation process does not become appreciable until temperatures increase beyond 6000°R. Note that the sublimation process yields appreciably greater amounts of triatomic carbon gas than monatomic carbon. Note also that, as the sublimation rate increases, the gas at the surface becomes saturated with the sublimation products, driving away the oxygen- and nitrogen-bearing species. At about 7400°R for this pressure, the sublimation process begins to induce pressure gradients in the gas normal to the gas-solid interface (Fig. 2).

Figure 10 shows the variation of the effective mass fractions of the elements carbon and nitrogen with surface temperature for several stagnation pressures. As seen in the previous figure, carbon monoxide is the only carbon-bearing species present in significant quantity at the surface for the lower temperatures i.e., $3000 < T_w < 5000$°R. In this temperature range (i.e., the diffusion-controlled oxidation regime),

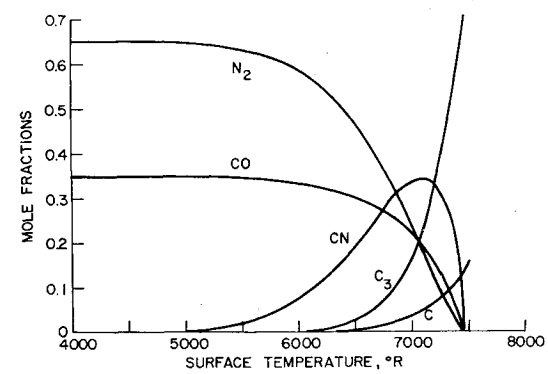

Fig. 9 Chemical composition at a graphite surface, $p = 1.0$ atm.

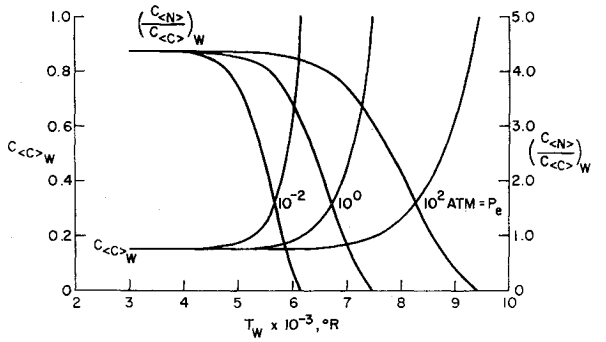

Fig. 10 Variation of elemental mass fractions with surface temperature and pressure.

$C_{(C)_w} = 0.15$. At higher surface temperatures, nitrogen reacts with the carbon surface, producing the cyano radical CN, sublimation of the solid graphite yields increasing amounts of atomic and triatomic gaseous carbon, and the effective mass fraction of the element carbon increases exponentially with surface temperature. The shift in $C_{(C)_w}$ with stagnation pressure has been found to be logarithmic, and the usefulness of this quantity in correlating the results will be demonstrated in the ensuing discussion. This physical quantity has the same variation with surface temperature and stagnation pressure as does the sublimation rate. Moreover, the driving force for the mass-transfer rate in the diffusion-controlled oxidation regime as well as in the diffusion-controlled sublimation regime is found to be related to $C_{(C)_w}$. The quantitative relationship between $C_{(C)_w}$, the surface temperature, and the stagnation pressure has been found to be given by

$$C_{(C)_w} = 0.15 + 2.4 \times 10^6 P_e^{-0.67} \exp[-11.1 \times 10^4/T_w] \quad (33)$$

where P_e is in atmospheres and T_w in °R.

In Fig. 10, one also can determine the conditions, which delimit the applicability of the present theory, i.e., when $C_{(C)_w} \to 1.0$. Beyond this point, a normal pressure gradient will be induced in the flow.

Figures 11–14 show typical boundary-layer concentration profiles and variations of the chemical source terms through the viscous layers for surface temperatures of 6500° and 7500°R at a stagnation pressure of 5.7 atm. A positive value of the chemical source term $\dot{w}_i$ indicates that the chemical species is being produced, whereas a negative value denotes that it is being consumed as a result of the chemical reactions. It is noted that the scaling of the chemical source terms in the stagnation regime must be as $R_B\dot{w}_i$ since, in Eqs. (8) and (10), the stagnation-point velocity gradient is assumed to be Newtonian:

$$du_e/dx = R_B^{-1}[2(P_e - P_\infty)/\rho_e]^{1/2} \quad (34)$$

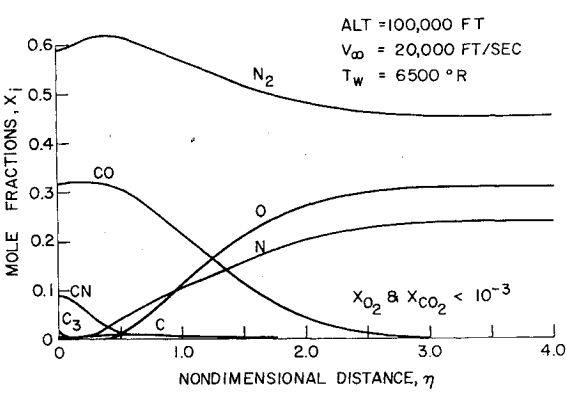

Fig. 11 Concentration profiles (T_w = 6500°R), equilibrium graphite sublimation.

At a surface temperature of approximately 5000°R, the mass loss mechanism is still one of diffusion-controlled oxidation, and the heterogeneous chemical reaction for this case is endothermic:

$$CO_2 + C(s) \to 2CO \qquad \Delta Q = 34 \text{ (kcal/mole)}$$
$$(T = 5000°\text{R}) \quad (35)$$

The composition profiles and associated homogeneous combustion reactions for this mechanism are discussed in Ref. 3.

Now, at a surface temperature of approximately 5500°R, nitrogen begins to undergo heterogeneous reactions directly with the surface to form CN. Also, for this surface temperature, multiple flame zones exist in the gas phase. At a slightly higher surface temperature ($T_w \sim$ 6000°R), one finds that the chemical reaction resulting in the formation of carbon monoxide has moved away from the surface. Also, one finds that additional CN is being produced in the first flame zone nearest the surface. At this surface temperature, therefore, the formation of CN is caused by both a heterogeneous and a homogeneous reaction, and the diffusion flux of this species is positive (i.e., away from the surface).

In the second flame zone from the surface, the major chemical reaction results in the formation of carbon monoxide through an exchange reaction between CN and O, and CO then diffuses back to the surface. Thus, the net mass flux of carbon monoxide at the surface is zero (i.e., $\dot{m}_{CO_w} = 0$), since its diffusion flux (j_{CO_w}) is identically equal and opposite to its convective flux ($C_{CO_w}\dot{m}_w$) [see Eq. (24)].

When the surface temperature increases to approximately 6500°R, the chemical reaction that results in the formation of CN begins to move away from the surface and into the gas phase. At this point, $\dot{m}_{CN_w} \cong 0$ since $j_{CN_w} \cong -(C_{CN_w})$. $(\dot{m}_{CN_w})$, and the mass loss mechanism is therefore entirely that caused by the vaporization reaction, which produces C_3. One notes that the chemical reaction in the first zone is endothermic as nitrogen is seen to react with the gaseous carbon species to form CN. In the second flame zone, the over-all energy change is exothermic, and one notes that carbon monoxide and atomic gaseous carbon are being formed, and they subsequently diffuse back to the surface (Figs. 11 and 12).

Figures 13 and 14 indicate the heterogeneous and homogeneous chemical interactions for a higher surface temperature (T_w = 7500°R) at the same hypersonic conditions as the two preceding figures. The corresponding normalized temperature and velocity profiles for these two surface temperatures are shown in Fig. 15. The temperature variation for T_w = 7500°R clearly shows the effect of the endothermic reaction and associated temperature reduction near

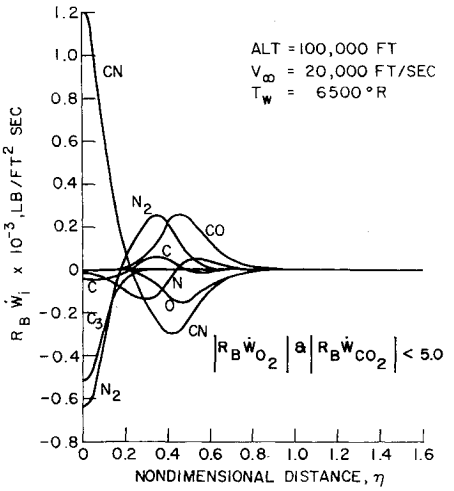

Fig. 12 Chemical source terms (T_w = 6500°R), equilibrium graphite sublimation.

the surface as well as the temperature overshoot resulting from the exothermic reactions occurring further out in the gas phase.

Figure 16 shows the variation of the normalized mass loss in the sublimation regime as a function of surface temperature and stagnation pressure. The normalizing factor is the diffusion-controlled oxidation mass-transfer rate. It is interesting to note that, if the gas model utilized for the diffusion-controlled oxidation regime in the earlier study had included the reactive chemical species CN in addition to CO and CO_2 as the ablation products, then the diffusion-controlled mass loss would not have "fallen off" slightly at the higher temperatures but would have remained at a constant level in this regime (see Fig. 18 of Ref. 3). Essentially, the quantity $\dot{m}_D(R_B/P_e)^{1/2}$ is independent of surface temperature and can be put into the form

$$\dot{m}_D(R_B/P_e)^{1/2} = 6.35 \times 10^{-3} \text{ lb/ft}^{3/2} \text{ sec-atm}^{1/2} \quad (36)$$

Note that $\dot{m}_S/\dot{m}_D$ in Fig. 16 ranges over five decades of stagnation pressure, includes surface temperatures up to 9500°R, and has the same variation with stagnation pressure and surface temperature as does the effective mass fraction (Fig. 10) of the element carbon at the surface. In fact, the results of a number of boundary-layer solutions covering a wide range of stagnation enthalpies, stagnation pressures, and surface temperatures yielded the relationship

$$\dot{m}_S/\dot{m}_D \cong 6.67 C_{\langle C \rangle_w} \quad (37)$$

When one combines the previous results (i.e., Ref. 3) for the low-temperature reaction-rate-controlled regime, the transition regime, and the diffusion-controlled oxidation regime with the new solutions given here for the sublimation regime, one obtains the results shown in Fig. 17.

In order to relate the low-temperature oxidation results to the new work presented here, it might be appropriate at this point to summarize briefly the oxidation theories peculiar to the reaction-rate-controlled and transition regimes. (For the details concerning these regimes, see Refs. 3 and 7–13.) Examination of the available experimental data indicates that, in the reaction-rate-controlled regime, the oxidation process follows a rate law, which may be written in the Arrhenius form as

$$\dot{m}_R = K_0 e^{-E/RT_w} (P_{O_2})_w^n \quad (38)$$

In this equation, $(P_{O_2})_w$ is the partial pressure of the oxygen at the surface, n is the order of the reaction, K_0 is the effective collision frequency, and E is the activation energy for the chemical reaction. The mass loss in this regime is noted to increase exponentially with surface temperature T_w. Depending upon the investigator, type of graphite studied, and the test conditions, the order of the reaction n has been reported to vary between zero and unity; the activation energy E falls within the limits 8 to 60 kcal/mole; the effective collision frequency can vary over several orders of magnitude. For our calculations, we have taken arbitrarily the order of the reaction to be one-half, the activation energy to be 44 kcal/mole, and we have chosen two values of K_0 that effectively bracket the existing experimental data (i.e., we arbitrarily choose the "fast" reaction rate, which is typical of the performance of ATJ-type graphites, whereas the pyrolytic-type graphite reaction rates are orders of magnitude slower, Fig. 17).

The different theories that exist for the variation of the mass loss through the transition regime are associated to

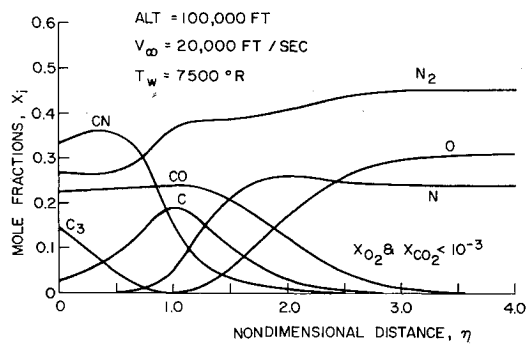

Fig. 13 Concentration profiles (T_w = 7500°R), equilibrium graphite sublimation.

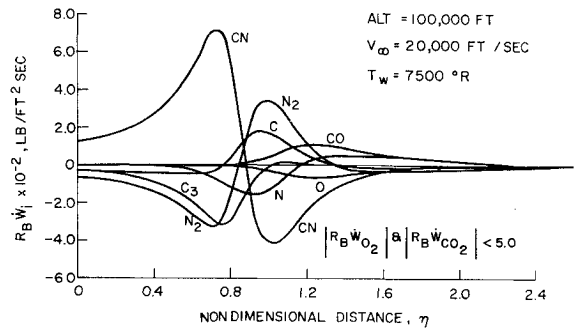

Fig. 14 Chemical source terms (T_w = 7500°R), equilibrium graphite sublimation.

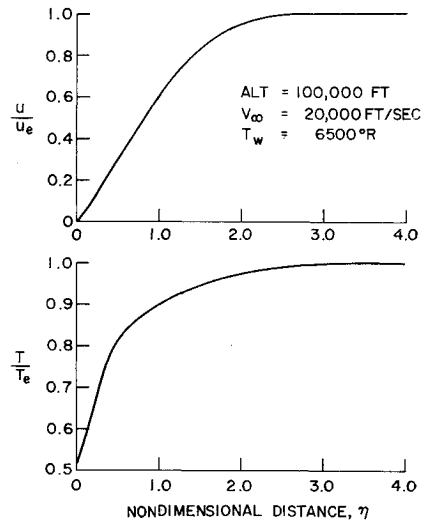

Fig. 15a Temperature and velocity profiles (T_w = 6500°R), equilibrium graphite sublimation.

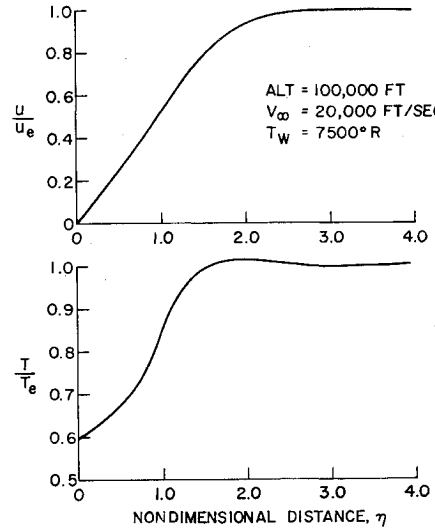

Fig. 15b Temperature and velocity profiles (T_w = 7500°R), equilibrium graphite sublimation.

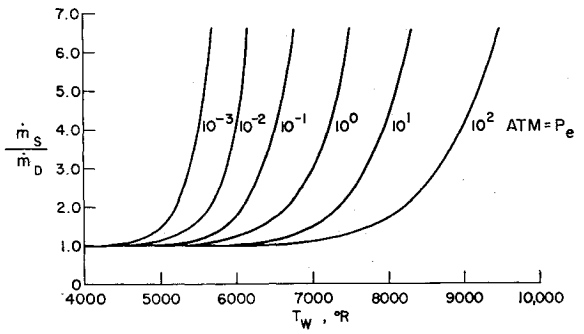

Fig. 16 Normalized graphite sublimation rate.

some degree with the concept of two resistances in series, one chemical and the second gas dynamic. The "double-plateau" theory[12,13] appears to be useful when applied to the situation of fast-reaction kinetics associated with the ATJ-type graphites. A second theory[3,6,24] is based on the fact that the diffusion-controlled mass transfer $\dot{m}_D$ varies as the square root of the stagnation pressure, and on the assumption that the reaction-rate-controlled mass loss $\dot{m}_R$ is based on one-half-order kinetics. The resulting equation, which Scala has derived for the variation of mass transfer through the transition regime, is shown as follows:

$$\dot{m} = \left[\frac{1}{\dot{m}_R{}^2} + \frac{1}{\dot{m}_D{}^2}\right]^{-1/2}$$

$$\text{or} \quad \frac{\dot{m}}{\dot{m}_D} = \left[1 + \left(\frac{\dot{m}_D}{\dot{m}_R}\right)^2\right]^{-1/2} \tag{39}$$

The normalized mass-transfer results for ablating graphite (shown in Fig. 17) now may be represented rather simply (for the entire range of surface temperatures) in terms of the effective mass fraction of the element carbon. Remembering that in the diffusion-controlled oxidation regime the plateau is given by $C_{\langle C\rangle_w} = 0.15$, one has, from Eq. (37),

$$\dot{m}/\dot{m}_D = C_{\langle C\rangle_w}/0.15 \tag{40}$$

Therefore, in the low-temperature reaction rate and transition regimes, $C_{\langle C\rangle_w}$ is given by

$$C_{\langle C\rangle_w} = 0.15[1 + (\dot{m}_D/\dot{m}_R)^2]^{-1/2} \tag{41}$$

and in the sublimation regime by Eq. (33).

Now substitute the value [Eq. (36)] of the diffusion-controlled mass-transfer rate into Eq. (40) and rearrange to obtain

$$\frac{\dot{m}_w}{C_{\langle C\rangle_w}}\left(\frac{R_B}{P_e}\right)^{1/2} = 0.04235 \ \frac{\text{lb}}{\text{ft}^{3/2}\ \text{sec-atm}^{1/2}} \tag{42}$$

It is interesting to compare the form of Eq. (42) with the results of an earlier vaporization study.[17] In Fig. 4 of Ref. 17, the quantity $\dot{m}_w R_B{}^{1/2}/C_{K_w}$ was represented as a function of the flight velocity, altitude, and surface temperature. There, C_{K_w} was defined to be the mass fraction of vaporizing

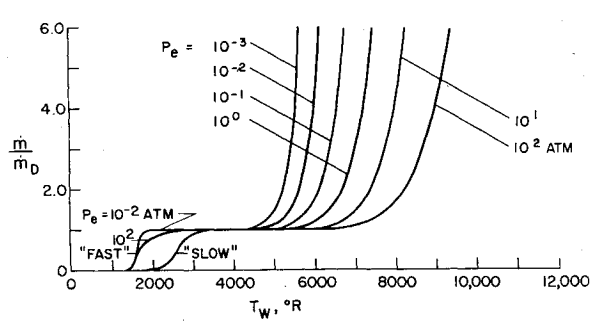

Fig. 17 Normalized hypersonic ablation rate of graphite over entire range of surface temperature.

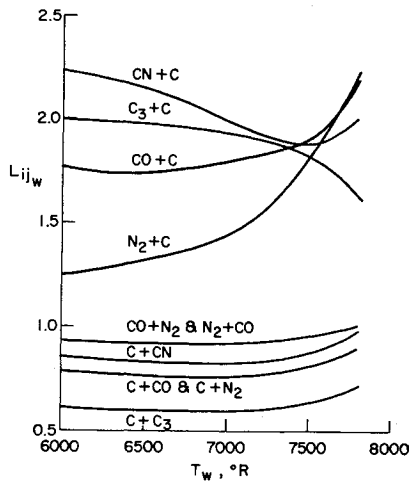

Fig. 18 Typical multicomponent Lewis numbers at surface of subliming graphite, p_e = 5.7 atm.

species injected into the boundary layer. Two correlation equations for $\dot{m}_w R_B{}^{1/2}/C_{K_w}$ were offered in that work that represented the data within 15 to 25%. Upon a re-examination of those earlier results, we now find that Eq. (42), given previously (with a proper interpretation of C_{K_w}), represents the data of Fig. 4 of Ref. 17 to within 10%. This very important result appears to indicate that the mass-transfer rates for arbitrary ablation systems for the hypersonic stagnation region may be approximated closely in a very simple manner, i.e., by the solution of a set of algebraic thermochemical equations which yields the quantity

$$\sum_k C_{\langle k\rangle_w}$$

The Lewis numbers of the gas mixture are defined[19] in terms of the multicomponent diffusion coefficients D_{ij} which, unlike the binary diffusion coefficients $\mathfrak{D}_{ij}$, are not symmetric. Therefore, in addition to being both temperature- and composition-dependent, the magnitude of the Lewis numbers depends upon the interactions of given pairs of particles in a nonsymmetric manner. It is clear that there are generally n^2-n values of the Lewis numbers; in this case there are 72, of which ten representative values are shown in Fig. 18.

Up to this point, we have considered only the mass-transfer phenomena. Now let us turn our attention to the heat transfer.[3,21,22,24,25] In the diffusion-controlled regime, the oxidation of graphite results in the formation of both CO and CO_2. The enthalpies of these species are negative with respect to those of undissociated air. The resulting energy change because of combustion is therefore exothermic, giving a positive contribution to the heat transferred to the surface. However, the thickening of the boundary layer because of mass transfer tends to reduce the heat transfer.

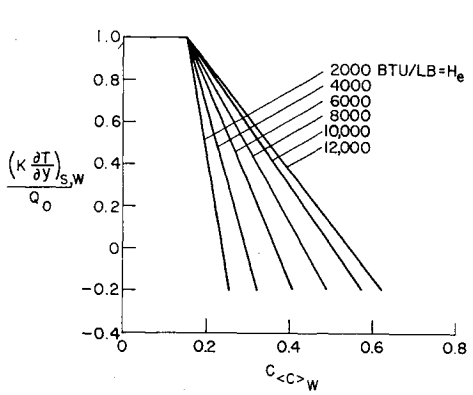

Fig. 19 Heat-transfer correlation for graphite sublimation.

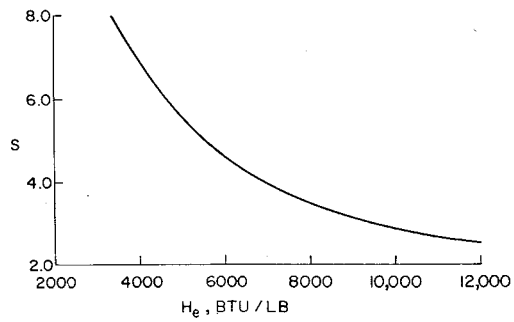

Fig. 20 Slope of reduction in heat-transfer rate in sublimation regime.

The net effect is to give a resultant energy flux into the solid that is nearly the same as the hypersonic heating in the absence of both combustion and mass transfer.

At higher surface temperature (i.e., the sublimation regime) the products of ablation include the species C, C_3, and CN. As noted in Fig. 8, the formation of these species necessitates an endothermic reaction causing a substantial reduction in the surface heating rate. These observations are indicated in the heat-transfer correlation shown in Fig. 19. Here, the heat conducted into the solid ablating graphite $(K\partial T/\partial y)_{s,w}$ is normalized by the heat-transfer rate in the diffusion-controlled oxidation regime Q_0 and plotted as a function of the effective mass fraction of the element carbon. The relationship between the diffusion-controlled heat transfer, the stagnation pressure, the nose radius, and the enthalpy difference across the boundary layer which was given in Ref. 3 is shown in the following:

$$Q_0(R_B/P_e)^{1/2} = 33.3 + 0.0333 \times [H_e - h_{w_{air}}] \text{ Btu/ft}^{3/2} \text{ sec-atm}^{1/2} \quad (43)$$

From an energy balance at the surface of ablating graphite including, in addition to the gas-phase conduction, diffusion and convection, the energy conducted into the surface layer of the condensed phase $K(\partial T/\partial y)_{s,w}$ is defined as

$$K\left(\frac{\partial T}{\partial y}\right)_{s,w} = \left(K\frac{\partial T}{\partial y} - \sum_i \rho_i V_i h_i\right)_{g,w} - \dot{m}_w(h_w - h_{C(s)}) \quad (44)$$

and, as such, does not include the effects of the forward radiation from the hot-gas cap or the surface reradiation. However, both of these quantities can be accounted for rather simply.

Now, when CO is the primary combustion product (as is the case in the diffusion-controlled oxidation regime), $C_{\langle C\rangle_w} = 0.15$, and $(K\partial T/\partial y)_{s,w} \equiv Q_0$. As the surface temperature rises and sublimation begins, the quantity $C_{\langle C\rangle_w}$ increases exponentially with surface temperature, as seen in Fig. 10. This is accompanied by the dramatic decrease in the heating rate shown in Fig. 19. The heat-transfer correlation equation for graphite ablation may be written as follows:

$$[(K\partial T/\partial y)_{s,w}/Q_0] = 1.0 - S(C_{\langle C\rangle_w} - 0.15) \quad (45)$$

where the slope S decreases with increasing stagnation enthalpy. The quantity S, shown in Fig. 20, has been curve-fitted as a fifth-degree polynomial in stagnation enthalpy shown in the following:

$$\left.\begin{aligned} S &= a + bH_e + cH_e^2 + dH_e^3 + eH_e^4 + fH_e^5 \\ a &= 1.868 \times 10^{1} \qquad d = 1.146 \times 10^{-12} \\ b &= -4.418 \times 10^{-3} \qquad e = -2.057 \times 10^{-15} \\ c &= 3.945 \times 10^{-7} \qquad f = 8.333 \times 10^{-20} \end{aligned}\right\} \quad (46)$$

A dimensionless quantity of interest in energy transfer phenomena is the Prandtl number. The Prandtl number of the gas mixture at the surface, defined[19] in terms of the specific heat, the viscosity, and the thermal conductivity of the gas, is shown in Fig. 21. The relationship between Pr_w and $C_{\langle C\rangle_w}$ is shown in Fig. 21, for a wide range of hypersonic conditions.

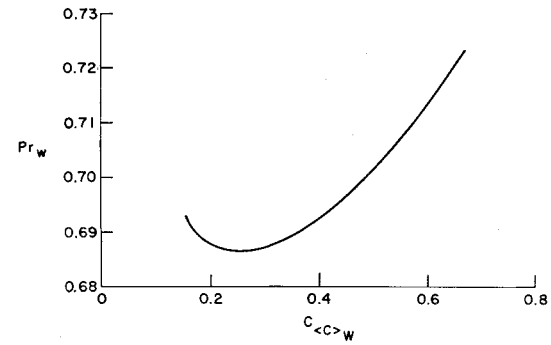

Fig. 21 Prandtl number of gas mixture at surface of subliming graphite.

A correlation parameter for the skin-friction coefficient in the presence of subliming graphite has been found which effectively reduces all of the data for a wide range of stagnation pressure, stagnation enthalpy, and surface temperature to a single curve. This parameter is shown in Fig. 22. This skin-friction correlation parameter may be expressed in a number of ways as shown in the following:

$$\frac{C_H B}{C_f} = \left(\frac{\dot{m}}{C_f}\right)_w \Big/ (\rho u)_e = \left(\frac{\dot{m}_w}{C_{f_w}}\right)\left(\frac{R_B}{x}\right)\frac{(\epsilon/2)^{1/2}}{\rho_\infty V_\infty} \quad (47)$$

where ϵ is the normal shock-density ratio.

In order to ascertain the relative importance of the chemical species present in the model representing the graphite sublimation process, additional computations were performed in which the magnitude of the mole fractions for CN and C_3 were reduced arbitrarily from their equilibrium values. This was done by reducing the equilibrium K_p function for CN [i.e., Eq. (20)] one order of magnitude and by reducing the K_p function for C_3 [i.e., Eq. (21)] three orders of magnitude (Fig. 23). Note that reducing X_{CN} one order of magnitude reduced the mass transfer by 24% but increased the heat-transfer rate by 146%. A reduction of X_{C_3} of three orders of magnitude resulted in a 32% reduction in the mass loss and an increase of 120% in the heat transfer. Interestingly enough, the relationships given by Eqs. (37) and (42) were still satisfied for these two "nonequilibrium" solutions. This would appear to suggest that the quantity $(\dot{m}/C_{\langle C\rangle})_w$ is the same for both equilibrium and nonequilibrium conditions. If this is the case, the nonequilibrium mass transfer may be estimated quite readily through an evaluation of the nonequilibrium surface concentrations. A general discussion of the theory of nonequilibrium vaporization processes as applied to hypersonic laminar boundary layers is given in Ref. 17.

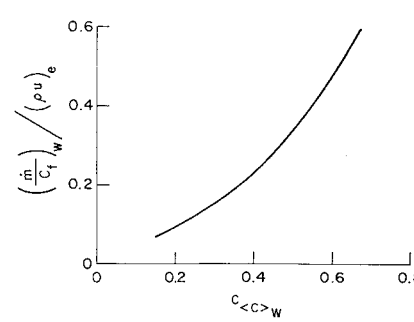

Fig. 22 Skin-friction correlation for graphite sublimation.

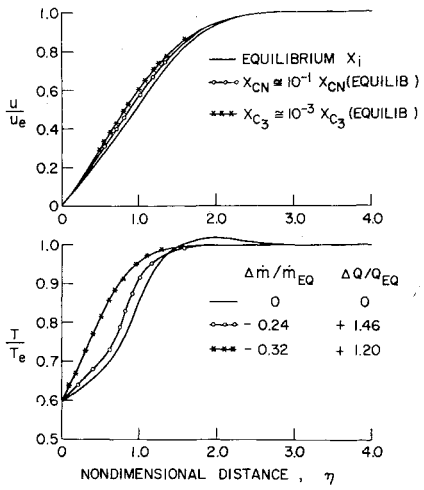

Fig. 23 Comparison of temperature and velocity profiles, alt = 100,000 ft, V_∞ = 20,000 fps, and T_w = 7500°R.

The effect of a change in the chemical model evidently produces a stronger net effect on the heat-transfer rate than on the mass-transfer rate. This occurs because not only is $C_{\langle C\rangle_w}$ itself affected by the choice of the chemical model but so is h_w, the enthalpy of the gas mixture at the surface that depends critically upon the gas composition through the heats of formation of the chemical species present. This, in turn, alters the driving enthalpy potential $H_e - h_w$, which produces a profound change in the heat-transfer rate.

VII. Conclusions

In a theoretical treatment of the vaporization of graphite in a hypersonic environment, it has been established that one must begin with a realistic chemical model in which one includes the contributions of dominant species such as C_3 and CN. If either of these species is not included in the model, the results would be seriously in error.

The mass-transfer rate has been correlated to the effective mass fraction of the element carbon at the surface. It has been shown that, over the complete range of surface temperatures, stagnation enthalpies and stagnation pressures of interest, the mass loss increases linearly with $C_{\langle C\rangle_w}$. In addition, it has been found that the heat-transfer rate into the surface also correlates, and at each value of the stagnation enthalpy, the heat-transfer rate decreases linearly with $C_{\langle C\rangle_w}$. The skin-friction coefficient likewise has been correlated and has shown to vary inversely with $C_{\langle C\rangle_w}$.

Finally, the range of validity of the present results has been established by determining the combination of surface temperatures and stagnation pressures for which the pressure gradient normal to the surface is significant, and the boundary-layer approximation is invalid.

References

[1] Scala, S. M., "Surface combustion in dissociated air," Jet Propulsion **28**, 340–341 (1958).

[2] Scale, S. M., "A study of hypersonic ablation," *Proceedings of the Tenth I.A.F. Congress* (Springer-Verlag, London, 1959), pp. 790–828.

[3] Scala, S. M., "The Ablation of graphite in dissociated air, Part I. Theory," IAS Paper 62–154 (June 1962); also General Electric Co., Missile and Space Division, Rept. TIS R62SD72 (September 1962).

[4] Scala, S. M., "The thermal protection of a re-entry satellite," ARS J. **29**, 670–672 (1959).

[5] Scala, S. M. and Nolan, E. J., "Aerothermodynamic feasibility of graphite for hypersonic glide vehicles," *Re-entry and Vehicle Design* (Academic Press, Inc., New York, 1960), Vol. 4, pp. 31–63.

[6] Nolan, E. J. and Scala, S. M., "Aerothermodynamic behavior of pyrolytic graphite during sustained hypersonic flight," ARS J. **32**, 26–35 (1962).

[7] Gulbransen, E. A. and Andrew, K. F., "Reactions of artificial graphite," Ind. Eng. Chem. **44**, 1034–1044 (1952).

[8] Parker, A. S. and Hottel, H. C., "Combustion rate of carbon," Ind. Eng. Chem. **28**, 1334–1341 (1936).

[9] Horton, W. S., "Oxidation kinetics of pyrolytic graphite," General Electric Co., General Engineering Laboratory Rept. 60GL218 (January 1961).

[10] Henning, G. R., "Surface oxides on graphite single crystals," *Proceedings of the Fifth Conference on Carbon* (Pergamon Press, New York, 1962), Vol. 1, p. 143–146.

[11] Arthur, J. R., "Reactions between carbon and oxygen," Trans. Faraday Soc., **47**, 164 (1951).

[12] Golovina, E. S. and Khaustovich, G. P., "The interaction of carbon with carbon dioxide and oxygen at temperatures up to 3000°K," *Eighth Symposium on Combustion* (Williams and Wilkins Co., Baltimore, Md., 1962), pp. 784–792.

[13] Welsh, W. E., Jr. and Chung, P. M., "A modified theory for the effect of surface temperature on the combustion rate of carbon surfaces in air," *Proceedings of the 1963 Heat Transfer and Fluid Mechanics Institute* (Stanford University Press, Stanford, Calif., 1963), pp. 146–159.

[14] Vidale, G. L., "The vaporization of graphite, TiC, Zrc, and HfC," General Electric Co., Missile and Space Division, Rept. TIS R61SD010 (January 1961).

[15] Denison, M. R. and Dooley, D. A., "Combustion in the laminar boundary layer of chemically active sublimators," Aeronutronic Systems Rept. U-110 (September 1957).

[16] Emmons, H. W. and Leigh, D., "Tabulation of the Blasius function with blowing and suction," Div of Applied Science, Combustion Aerospace Lab., Harvard Univ., Interim TR 9, (November 1953).

[17] Scala, S. M. and Vidale, G. L., "Vaporization processes in the hypersonic laminar boundary layer," *Int. J. Heat and Mass Transfer* (Pergamon Press, New York, 1960), Vol. 1, pp. 4–22.

[18] Scala, S. M., "Vaporization of a refractory oxide during hypersonic flight," *1959 Heat Transfer and Fluid Mechanics Institute* (Stanford University Press, Stanford, Calif., 1959), p. 181.

[19] Hirschfelder, J. O., Curtiss, C. F., and Bird, R. B., *Molecular Theory of Gases and Liquids* (John Wiley and Sons, Inc., New York, 1954).

[20] Scala, S. M., "The equations of motion in a multicomponent chemically reacting gas," General Electric Co., Missile and Space Division, Rept. TISR58SD205 (December 1957).

[21] Lees, L., "Convective heat transfer with mass addition and chemical reactions," *Third AGARD Colloquium on Combustion and Propulsion* (Pergamon Press, Inc., New York, 1959).

[22] Scala, S. M. and Gilbert, L. M., "Theory of hypersonic lamina stagnation region heat transfer in dissociating gases," *Developments in Mechanics: Proceedings of the Eighth Midwestern Mechanics Conference*, edited by S. Ostrach (Pergamon Press, Inc., New York, May 1965); also General Electric Co., Missile and Space Division, Rept. TIS R63SD40 (April 1963).

[23] Cook, C. A., Gilbert, L. M., and Scala, S. M., "Normal shock waves in air at flight speed up to 25,000 ft./sec.," General Electric Co., MSD, Rept. TIS R62SD76 (November 1962).

[24] Scala, S. M. and Gilbert, L. M., "Aerothermochemical behavior of graphite at elevated temperatures," General Electric Co., Missile and Space Division, Rept. TIS R63SD89 (November 1963).

[25] Fay, J. A. and Riddell, F. R., "Theory of stagnation point heat transfer in dissociated air," J. Aero space Sci. **25**, 78–85 (1958).